Science of the Total Environment 749 (2020) 142385

Contents lists available at ScienceDirect

Science of the Total Environment

journal homepage: www.elsevier.com/locate/scitotenv

An efficient and simple method using a graphite oxide electrochemical sensor for the determination of glyphosate in environmental samples

Jaqueline S. Santos [a,b], Montcharles S. Pontes [a], Etenaldo F. Santiago [a], Antonio R. Fiorucci [b], Gilberto J. Arruda [b,*]

[a] Department of Plant Resources, Natural Resources Program (PGRN), Mato Grosso do Sul State University (UEMS), P.O. Box 351, Dourados, MS 7984-970, Brazil
[b] Department of Analytical Chemistry, Natural Resources Program (PGRN), Mato Grosso do Sul State University (UEMS), P.O. Box 351, Dourados, MS 7984-970, Brazil

HIGHLIGHTS

- Direct electrochemical determination of glyphosate in environmental samples
- Simple and efficient sensor based on graphite oxide
- The developed sensor had higher ease of oxidation of glyphosate, with a current gain of 363% compared to CPE.
- Precision, repeatability, and selectivity of the sensor indicate high analytical performance.

GRAPHICAL ABSTRACT

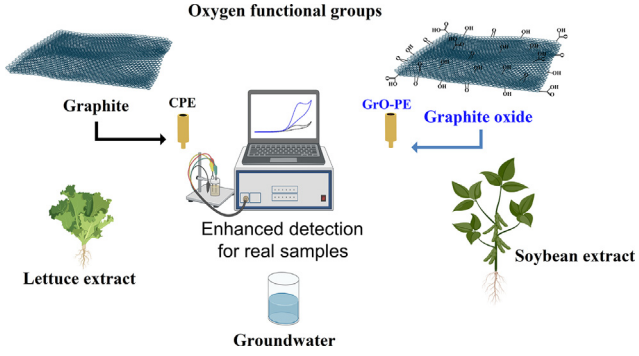

ARTICLE INFO

Article history:
Received 6 July 2020
Received in revised form 10 September 2020
Accepted 11 September 2020
Available online 17 September 2020

Editor: Damia Barcelo

Keywords:
Electrochemical sensor
Voltammetry
Glyphosate determination
Groundwater samples
Soybean and lettuce extract

ABSTRACT

Excessive and indiscriminate use of the herbicide glyphosate (GLY) leaves the environment susceptible to its contamination. This work describes the development of a simple, inexpensive, and efficient electroanalytical method using graphite oxide paste electrode (GrO-PE) for the direct determination of GLY traces in groundwater samples, soybean extracts, and lettuce extracts. Under optimal experimental conditions, the developed sensor exhibited a linear response of the peak current intensity *vs.* the concentration, in the range of 1.8×10^{-5} to 1.2×10^{-3} mol L^{-1} for GLY. The limits of detection and quantification are 1.7×10^{-8} mol L^{-1} and 5.6×10^{-8} mol L^{-1}, respectively. The methodology developed here demonstrated a strong analytical performance, with high reproducibility, repeatability, and precision. Moreover, it successfully avoided interference from other substances, showing high selectivity. The GrO-PE sensor was effectively applied to determine GLY traces in real samples with recovery rates ranging from 98% to 102%. Results showed that the GrO-PE is effective and useful for GLY detection, with the advantage of not involving laborious modifications and complicated handling, making it a promising tool for environmental analysis.

1. Introduction

Herbicides are chemical compounds widely used in agriculture to control weeds (Habekost, 2014). Among the most traded in the world is glyphosate [N-(phosphonomethyl) glycine] (GLY) (Van Stempvoort et al., 2014), a non-selective, broad-spectrum systemic herbicide (Yang et al., 2019), which acts by inhibiting the activity of the 5-enolpyruvylshikimate-3-phosphate synthase (EPSPS), that is present in plants, fungi, and bacteria but absent in animals (Kishore and Shah, 1988; Santos et al., 2020). In plants, the blockade of the shikimate route causes the accumulation of shikimic acid (Zelaya et al., 2011; Franco et al., 2012), reducing the biosynthesis of aromatic amino acids and some metabolites until the death of the organism (Johansson et al., 2018).

* Corresponding author.
E-mail address: arruda@uems.br (G.J. Arruda).

https://doi.org/10.1016/j.scitotenv.2020.142385
0048-9697/

GLY is inactivated by sorption in the topsoil (Bento et al., 2016), and microorganisms are mainly responsible for its degradation (Okada et al., 2016). However, due to the continuous use of this herbicide, the sorption and degradation mechanisms have not prevented the contamination of deeper layers of soil (Do et al., 2015). Thus, GLY has often been detected in surface water and groundwater (Zhao et al., 2018); its typical half-life in soil and surface water is in the range of 2 to 215 days and 2 to 91 days, respectively (Berman et al., 2018). However, this degradation time can vary due to physical, chemical, and biological factors such as temperature, luminosity, microbiota, nutrients, salinity, and pH (Mercurio et al., 2014; Bento et al., 2016).

Given the persistence of GLY in the environment and the possible resulting damages, many analytical methods have been developed for its determination; the chromatographic methods are most commonly described in the literature (Cao et al., 2019), which highlights high-performance liquid chromatography (Bernal et al., 2010; Zhang et al., 2013) and gas chromatography (Royer et al., 2000; Motojyuku et al., 2008). Despite the sensitivity and stability of the chromatographic methods, the high cost of the equipment and the laborious previous treatment of the samples (Moraes et al., 2010) hinder the widespread use of this technology (Sato et al., 2001). Therefore, electroanalytical methods using electrochemical sensors appear as a simple, economical, and efficient alternative to determine GLY traces; even less popular when compared to chromatography but no less effective. The development of electrochemical sensors with increasingly improved methods in relation to sensitivity and selectivity has gradually increased in recent years (Cao et al., 2019).

Among the sensors described in the literature are unmodified carbon paste electrodes (CPE) (Oliveira et al., 2018), glassy carbon electrode (GCE) modified by a core-shell structure based on polyaniline and multi-walled carbon nanotubes (MWCNT) (Moraes et al., 2010), Cu°-GCE obtained from electro crystallization of Cu° onto a surface of GCE (Aguirre et al., 2019), and a sensor based on pencil graphite electrode (PGE) modified by hollow fiber pregnant by MWCNT-ionic liquid composite and copper oxide nanoparticle (Gholivand et al., 2018). Other works describe a screen-printed sensor modified with gold nanoparticles (Xu et al., 2017), a double-template imprinted polymer nanofilm-modified PGE (Prasad et al., 2014), and a sensor based on molecularly imprinted polypyrrole-modified gold (Zhang et al., 2017).

Graphite oxide (GrO) is a precursor to graphene, with an electrical and thermal conductivity that can enhance the performance of electrochemical sensors by introducing certain chemical functional groups (Ping et al., 2012; Ping et al., 2014; Yao et al., 2019; Gurzęda et al., 2020). In this context, GrO has a layered structure containing oxygen atoms, which can form functional groups such as carboxyl and hydroxyl, causing an increase in the adsorptive properties of the material. GrO can be produced by the chemical oxidation of graphite (Gr), which causes defects in the basal plane of the material, favoring high electrochemical activity (Ping et al., 2011; Gao et al., 2014; Ping et al., 2015; Yao and Ping, 2018; Wong et al., 2019).

This research proposes a simple and inexpensive electrochemical sensor prepared from GrO for the direct determination of GLY in environmental samples. Cyclic voltammetry (CV) and square wave voltammetry (SWV) were employed to investigate the interactions between GLY and the sensor surface. Furthermore, transport properties on the sensor surface were investigated by electrochemical impedance spectroscopy (EIS). Finally, under optimized experimental and instrumental conditions, the new method developed was able to be practically and efficiently applied in determining GLY in samples of groundwater samples, soybean leaf extract, and lettuce leaf extract.

2. Materials and methods

2.1. Reagents and apparatus

Distilled water was the solvent used for the preparation of all solutions, and all reagents were analytical grade. The analyte was GLY (*N*-phosphonomethyl glycine, Sigma-Aldrich 99.2% w/w). Britton-Robinson (BR) buffer at a concentration of 0.2 mol L^{-1} was used as a supporting electrolyte. In the preparation of the supporting electrolyte, solutions of H_3PO_4, H_3BO_3, and CH_3COOH were used; to adjust its pH, adequate amounts of NaOH (0.2 mol L^{-1}) were added. A pH-meter (Hanna Instruments HI-3221) was used to measure the pH of the solutions.

Electrochemical measurements were performed at room temperature (25 ± 1 °C) using a PGSTAT128N Autolab potentiostat/galvanostat (Ecochemie, Utrecht, The Netherlands) controlled with NOVA 1.11 software. All measurements were taken with a conventional three-electrode system, using Ag/AgCl (3.0 mol L^{-1} KCl) as a reference electrode, a platinum wire as a counter electrode, and CPE and graphite oxide paste electrodes (GrO-PE) as working electrodes. The system mounted in the electrochemical cell was placed in a Faraday cage to minimize background noise. After each voltammogram recording, the surface of the working electrode was renewed and smoothed on a sheet of bond paper. This procedure was carried out to eliminate possible products adsorbed by the oxidation of GLY on the electrode surface. SWV and CV served as the voltammetric techniques used to investigate the electrochemical behavior of GLY on the surface of the working electrodes (CPE and GrO-PE).

2.2. Functionalization of Gr and development of working electrodes (CPE and GrO-PE)

The methodology used to functionalize Gr was adapted from the methodology described by William et al. (1958). Briefly, 5 g of Gr powder (Sigma-Aldrich; size particle < 20 μm) was dispersed in 100 mL of concentrated H_2SO_4 (Dynamic, 96%); this mixture was shaken (800 rpm) for 12 h at a temperature of 70 °C. The mixture was then filtered through a filter membrane (0.42 μm) using a vacuum pump (Prismatec model BBV-132). Successive filtrations using distilled water were performed until the pH approached neutrality; the precipitate obtained was then oven-dried at 105 °C for 12 h. The GrO resulting from the above process was used in the GrO-PE sensor.

A CPE was also prepared to compare functionalized and non-functionalized Gr. In the preparation of electrodes pastes, it was used for the CPE (70%/30% (w/w) Gr/paraffin) and for the GrO-PE (70%/30% (w/w) GrO/paraffin). These mixtures were macerated for 15 min and then heated for 10 min at 70 °C until the paraffin wax (Sigma-Aldrich) fused with Gr or GrO; the two pastes obtained were each immediately inserted into a 1.0 mL plastic syringe, with a geometric area of 7.73×10^{-2} cm^2. Electrical contact was established *via* a copper wire. The process of obtaining the GrO and fabrication of the electrochemical sensors are described in Scheme 1.

2.3. Characterization of Gr and GrO

Before and after functionalization, the Gr was characterized by the JSM-6380LV field-emission scanning electron microscope (SEM) (JEOL, Tokyo, Japan) equipped with an energy dispersive spectroscopy (EDS) module. The samples were coated with ultrafine gold to ensure the microstructures could be visualized; they also received an acceleration potential of 20 kV while the micrographs were created. Moreover, Fourier transform infrared spectroscopy (FTIR), performed on a Shimadzu IRA Affinity spectrophotometer, using a KBr pellet, was also used to examine these materials. The thermal gravimetric analysis (TGA) was performed in a TGA thermal analyzer, model 444 F3 Jupiter (Netzsch, Selb, Germany), in a Pt/Rh crucible under an inert atmosphere of nitrogen (gas flow: 20 mL min^{-1}) (results presented in Supplementary material, Topic 1.1, Figs. S1 and S2).

2.4. pH study, optimization of SWV parameters, and constructing the analytical curve

Using the GrO-PE, the SWV parameters were optimized in the presence of 5.4×10^{-5} mol L^{-1} of GLY, within a range of 5 to 80 Hz, 5 to

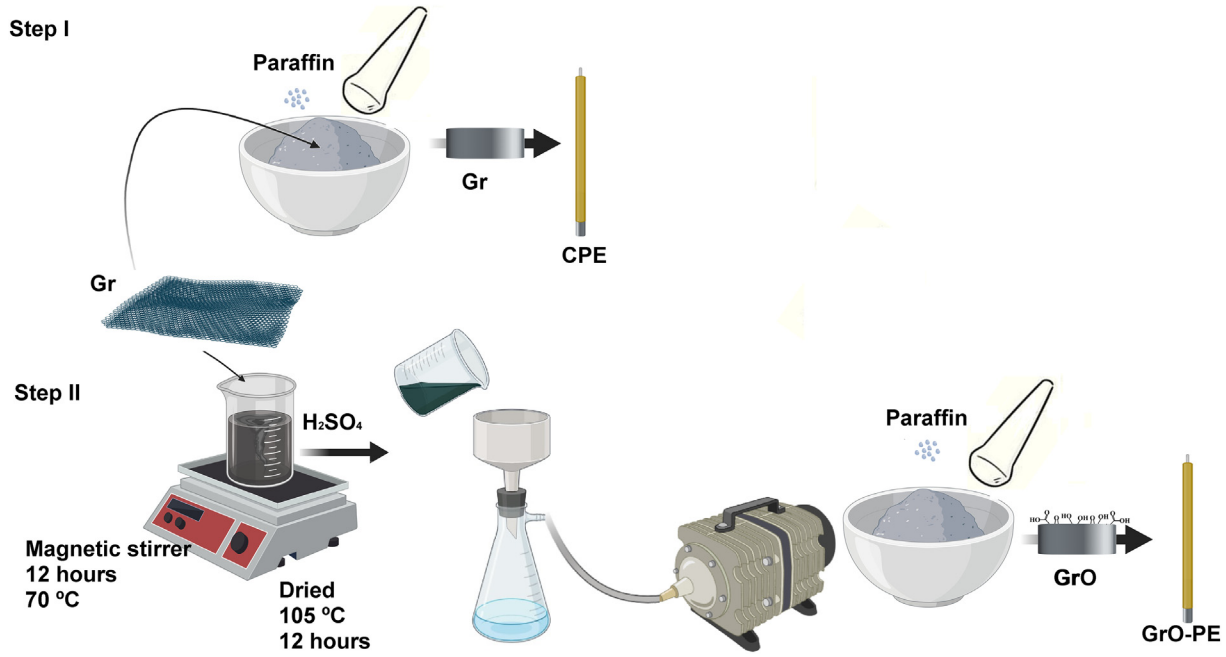

Scheme 1. Schematic representation of sensors preparation. CPE (step 1). GrO-PE (step 2).

60 mV, and 1 to 13 mV, of frequency, amplitude, and step potential, respectively. The effect of pH on the electrochemical behavior of GLY was studied by varying the pH between 4.0 and 8.0 in a GLY concentration of 99.37×10^{-6} mol L^{-1}. The scans were performed in the potential range of 0.90 to 1.40 V at a scan rate of 125 mV s^{-1}. These parameters were optimized while considering the higher peak current (I_p) values of oxidation of GLY. The peak potential (E_p) was also considered in the pH study.

The analytical curve was obtained in the concentration range of 1.8×10^{-5} to 1.2×10^{-3} mol L^{-1} for GLY, in a potential range of 0.8 to 1.6 V (*vs.* Ag/AgCl). The limit of determination (LOD) and limit of quantification (LOQ) were calculated using this curve following the recommendations of the International Union of Pure and Applied Chemistry (IUPAC, 1987). These recommendations suggest that LOD should equal $(3 \times sd) / s$ and LOQ equal $(10 \times sd) / s$, where s is the slope of the analytical curve and sd is the standard deviation of the intercept.

2.5. Precision, repeatability, reproducibility, and selectivity

The precision, repeatability, reproducibility, and selectivity of the sensor were estimated by analyzing I_p and E_p for GLY (7.2×10^{-6} mol L^{-1}) + extract (3 mg mL^{-1}), running measurements at six different times at the same day (precision), executing 20 consecutive measurements (repeatability), and using three sets of identical composition electrodes (reproducibility). Interference studies were conducted to acquire information on the selectivity of GrO-PE in the presence of potential interferents. The pesticides glufosinate, carbaryl, bentazon, monocrotophos, thiram, and carbofuran along with two degradation products of GLY (GDP), aminomethylphosphonic acid (AMPA) and sarcosine, were tested as likely interferents at a ratio of 1:1 (GLY: pesticides) and 1:1 (GDP). In addition, the specific ions Mn^{4+}, Fe^{2+}, Fe^{3+}, K^+, Cl^-, Zn^{2+}, SO_4^{2-}, BO_3^{3-}, Na^+, NO_3^-, PO_4^{3-}, and Ca^{2+} were simultaneously tested at a proportion of 1:30 (GLY: ions). After the addition of the interferents, the SWV voltammograms were obtained to evaluate the I_p and E_p oxidation values of GLY. The criterion used to choose the ions and other interferents was the probability of their presence in the investigated samples, since pesticides and GDP can be found in groundwater and plants, and many ions are plant nutrients.

2.6. Preparation and quantification in environmental samples

The method developed using GrO-PE was applied to environmental samples susceptible to GLY contamination. The matrices analyzed were groundwater, soybean (*Glycine max*) leaf extracts, and lettuce (*Lactuca sativa*) leaf extracts. All samples were acquired in Dourados, an agricultural city in Mato Grosso do Sul, a western province in Brazil. The groundwater (captured from a 70 m artesian well) was collected from a tap at the Campus of the State University of Mato Grosso do Sul. The hydroponic lettuce was purchased in the market, and the soybean was collected on a plantation. The soybean and lettuce extracts were obtained from 300 mg of leaves of the third node, using the center parts of the leaves and discarding the leaf ribs. This plant mass for each extract was macerated in 10 mL of BR buffer 0.2 mol L^{-1} (pH 6.0). Both extracts were filtered through a filter membrane (0.42 μm) using a vacuum pump. All samples were prepared and analyzed in triplicate.

Initially, to check the presence or absence of GLY, voltammograms were performed on the groundwater samples and plant extracts, confirming the absence of GLY. The method of standard addition was then used to quantify GLY levels in the samples. Thus, 25 μl aliquots of each matrix studied were spiked with 4.9×10^{-7} mol L^{-1}; 9.3×10^{-7} mol L^{-1}, and 19.2×10^{-7} mol L^{-1} of GLY, the 10 mL volume was completed with 0.2 mol L^{-1} BR buffer at pH 6.0 and SWV voltammograms were obtained to analyze the recovery amounts using the proposed method.

3. Results and discussion

3.1. The electrochemical characterization of CPE and GrO-PE

The electroactive area and the electric properties of transport in the double layer of the working electrodes were investigated using CV and EIS as an electrochemical method to determine the influence of electrodes surface functionalization. To stabilize the electrode-solution interface, a 5.0×10^{-3} mol L^{-1} solution of $[K_4[Fe(CN)_6]]/[K_3[Fe(CN)_6]]$ in 0.5 mol L^{-1} KCl was used. The reversibility of the electrochemical reaction between the Fe^{3+}/Fe^{2+} ions on the surface of the working electrode was evaluated by examining the relationship between the I_p

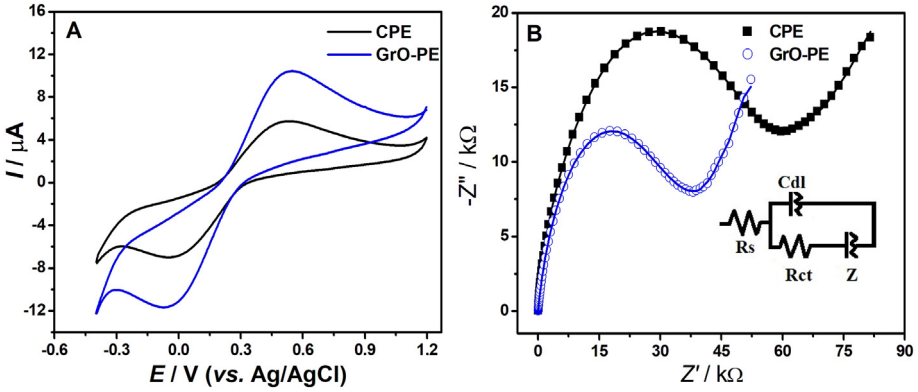

Fig. 1. (A) CVs reading, $v = 0.1$ V s^{-1}. (B) EIS spectra. $[K_4[Fe(CN)_6]]/[K_3[Fe(CN)_6]] = 5 \times 10^{-3}$ mol L^{-1} in KCl 0.5 mol L^{-1}.

(I_{pa}/I_{pc}) values determined from the voltammograms. Fig. 1A shows the voltammograms CV obtained using the CPE and GrO-PE electrodes. The ratio between the I_{pa}/I_{pc} values was approximately one for both electrodes, suggesting the reversibility of the Fe^{3+}/Fe^{2+} redox reaction on the surface of the working electrode. The working electrodes electroactive areas CPE (Fig. S3a, Supplementary material) and GrO-PE (Fig. S3b, Supplementary material) are calculated using the slope of the I_p *vs.* $v^{1/2}$ curves (Fig. S3c, Supplementary material); the results obtained are shown in Table 1. The obtained values showed that the GrO, when incorporated into the working electrode GrO-PE, increases the electrochemical area by more than 2.5 times compared to the CPE values. This gain causes an increase in the catalytic activity of the working electrode during the oxidation of the Fe^{3+}/Fe^{2+} on its surface.

To investigate the electrocatalytic performance of the electrode-solution interface, the double-layer capacitance (C_{dl}), solution resistance (R_s), and charge transfer resistance (R_{ct}) of the working electrodes CPE and GrO-PE were evaluated. For this purpose, experiments using EIS were performed; their results are presented in Fig. 1B and in Table 1. The parameters R_s, R_{ct}, and C_{dl} were determined by modeling the experimental results, utilizing the Nyquist diagram with a modified Randles equivalent circuit, as shown in Fig. 1B (Cesarino et al., 2011). According to the data obtained (Table 1), the GrO-PE decreased by approximately 30% and 62% compared to the CPE for R_s and R_{ct}, respectively. Considering the C_{dl} values, the results showed a 500% increase for GrO-PE when compared to the CPE. These results indicate an increase in the number of charges on the surface of the GrO-PE. In addition, the observed increase for the C_{dl} parameter may be related to a larger electrochemical reactive area due to the presence of GrO. The roughness factor (*RF*), was calculated (Table 1) by the ratio between these two areas (Petroni et al., 2017), showing an increase in *RF* values for the GrO-PE sensor. This increased roughness may have facilitated the interaction of GLY with the GrO-PE at the electrode-solution interface. The apparent standard rate constant ($k°$) was calculated using the ratio $k° = RT / F^2 R_{ct} AC$ (Cesarino et al., 2011), with, $k°$ showing an increase of approximately 60% for the GrO-PE sensor, indicating that the GrO facilitates the reaction of the Fe^{3+}/Fe^{2+} redox pair.

3.2. Electrochemical behavior of GLY using CPE and GrO-PE

The cyclic voltammograms obtained for both the working electrodes CPE and GrO-PE using a 0.2 mol L^{-1} BR buffer solution at pH 6.0 in the absence and presence of 3.5×10^{-4} mol L^{-1} of GLY are shown in Fig. 2. The voltammograms obtained only with the buffer in the absence of GLY did not display any peaks, indicating that no oxidation or reduction processes had occurred on the surface of both working electrodes and thus identifying the potential range that could be adopted to investigate the redox process of the GLY on the surface of the working electrodes. The voltammograms obtained when GLY was present in the electrochemical cell, presented an oxidation peak in the potential range of 0.80 to 1.45 V for both working electrodes.

The values obtained for E_p (V)/I_p (μA) were 1.26/2.77 and 1.31/13.18 when the CPE and GrO-PE electrodes were respectively used. The oxidation peak of the GLY displayed in the voltammograms for both working electrodes (Fig. 2) may be attributed to the irreversible oxidation of the secondary amine (Gholivand et al., 2018). When compared to the CPE, the GrO-PE subtly changed the E_p, with a displacement of approximately 50 mV. Concerning the I_p value, the GrO-PE demonstrated a current increase of 363% in comparison to the CPE, indicating higher ease of oxidation of GLY on the surface of GrO-PE. This could be related to the formation of oxygen-containing groups in its structure (*e.g.* carboxyl, hydroxyl, and epoxide) caused by the oxidation of Gr, thus increasing the catalytic activity of the GrO-PE (Gao et al., 2014). The increase in catalytic activity when protonated GLY is present in the electrochemical cell can be attributed to a greater chemical affinity between nitrogen atoms previously protonated with oxygen atoms that had been incorporated into Gr during functionalization, which consequently increased the sensitivity of this sensor.

3.3. Influence of pH

Using the GrO-PE as a working electrode, the effect of pH on the electrochemical behavior of GLY was investigated by SWV under optimal conditions: an *f* (frequency) of 25 Hz, step potential of 5 mV, and amplitude of 20 mV (Fig. S4, Supplementary material). As the pH increased, the E_p values changed to more negative values (Fig. S4b), indicating

Table 1
Calculated areas and EIS measurements obtained for CPE and GrO-PE (n = 3).

Electrode	Area [average ± SD] (10^{-2} cm^{-2})	*RF*	R_s [average ± SD] (Ω)	R_{ct} [average ± SD] (kΩ)	C_{dl} [average ± SD] (μF)	$k°$ [average ± SD] (10^{-5} cm s^{-1})
CPE	8.55 ± 0.09	1.11	29.51 ± 1.03	29.99 ± 0.88	0.37 ± 0.07	2.31 ± 0.99
GrO–PE	21.41 ± 0.44	2.77	22.47 ± 0.48	18.53 ± 0.77	1.83 ± 0.14	3.74 ± 1.15

SD: standard deviation. $A_{geometric} = 7.73 \times 10^{-2}$ cm^2. *RF* (roughness factor) = $A_{electrochemical}$ / $A_{geometric}$.

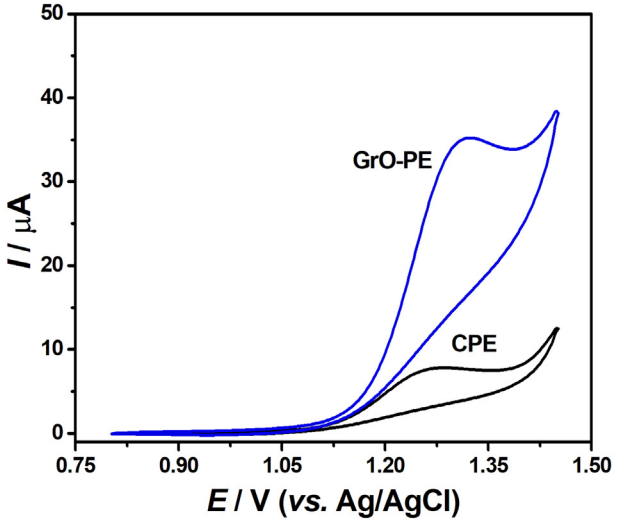

Fig. 2. CVs. Experimental conditions: [GLI] = 3.5×10^{-4} mol L^{-1}. v = 0.2 V s^{-1}. [BR] = 0.2 mol L^{-1}. pH = 6.0.

the intervention of protons in the electrochemical process of GLY in the working electrode GrO-PE, which demonstrates that the GLY oxidation is pH-dependent.

The linear relationship between the E_p and pH (Fig. S4b, Supplementary material) was shown by the regression equation of E_p (mV) = 1.520 ± 8–60 ± 2 pH, r = 0.998, with the slope of 60 ± 2 mV. The value obtained of 60 mV for the slope of the E_p *vs.* pH plot suggests protons participate in the oxidation reaction of GLY on the surface of the working electrode because this value approaches the one predicted by the Nernst equation (59 mV). It is important to note that the value obtained for the slope suggests equality in the number of protons and electrons involved in the redox process of the GLY on the surface of the GrO-PE. Fig. S4b, Supplementary material, shows the variation in I_p relative to the increase in pH. The increase of I_p is observed until pH 6.0; after this, a decrease of I_p is observed. The deprotonation of GLY as a compound with four acidic groups (pKa_3 5.6) (Sprankle et al., 1975) is pH-dependent. In the more acidic media, the functional groups present in the GLY molecule are protonated, which reduces its complexation ability (Gholivand et al., 2018). Thus, a pH of 6.0 was selected to investigate the electrochemical oxidation behavior of GLY on the surface of the working electrodes and to develop the electrochemical quantification methodology as applied to the samples examined (groundwater and leaf extracts from soybean and lettuce).

3.4. Influence of scan rate

The influence of the scan rate on I_p and E_p can be used as a diagnostic criterion to determine the electron transfer steps that occur on the electrode surface and clarify the mechanism of the redox process of the investigated compound. In this investigation, effects of the scan rate (v) on the electrochemical response of 4.5 × 10^{-4} mol L^{-1} GLY in 0.2 mol L^{-1} BR buffer at pH 6.0, using CPE and GrO-PE working electrodes were studied by CV. The range of ν used for this purpose were 0.025; 0.050; 0.075; 0.100; 0.125; 0.150; 0.175 and 0.200 V s^{-1} (Fig. S5a and b, Supplementary material). The I_p value was proportional to the scan rate in the range evaluated for both the CPE and GrO-PE electrodes (Fig. S5c, Supplementary material) and can be expressed as follows: I_p (μA) = 0.40 ± 0.03 + 12.75 ± 0.29 v (V s^{-1}), r = 0.99 for CPE and I_p (μA) = 1.69 ± 0.10 + 52.46 ± 0.84 v (V s^{-1}), r = 0.99 for GrO-PE. These results suggest that in the electron transfer process, adsorption may occur on the surface of the working electrode. The correlation between the log of I_p *vs.* log of v (Fig. S5d, Supplementary material) was calculated to confirm the adsorption step. This calculation demonstrated a linear relation represented by the following equations: log I_p (μA) = 0.95 ± 0.05 + 0.72 ± 0.08 log v (V s^{-1}), r = 0.98 and log I_p (μA) = 1.58 ± 0.03 + 0.73 ± 0.05 log v (V s^{-1}), r = 0.99, for CPE and GrO-PE respectively. The angular coefficient obtained in this relation, around 0.73, suggested that there is an adsorption step on the surface of the working electrodes (Greef et al., 1985).

3.5. Kinetic parameters n, H^+, Γ, and k_s

As shown above, in the influence of scan rate, the electrochemical process that occurs on the surface of the working electrodes (CPE and GrO-PE) is controlled by adsorption; for this type of reaction, the kinetic parameters n (number of electrons involved), H^+ (number of protons), Γ (surface coverage, in mol cm^{-2}), α (charge transfer coefficient), C (concentration, in mol cm^{-3}), and k_s (standard heterogeneous rate constant) can be experimentally determined (Kissinger and Heineman, 1983; Velasco, 1997). In determining the kinetic parameters, the following variables were used: E_p (in volt), peak potential at half height ($E_{p0.5}$, in volt), peak current at half height ($I_{p0.5}$, in amperes), charge consumed (Q, in coulomb), the Faraday constant (F), the gas constant (R), the temperature (T) in 298 K, the electrode area (A) in cm^2, and the scan rate (ν) of 0.20 V s^{-1}.

The value of n involved in the electrochemical oxidation of GLY on the surface of the working electrodes was estimated using Eq. (1), with values obtained of 2.19 ± 0.07 and 2.06 ± 0.09 for CPE and GrO-PE respectively. These values suggest that two electrons participate in the oxidation of GLY on the surface of both working electrodes. The value of H^+ was estimated using Eq. (2), the slope of Fig. S4b, Supplementary material (E_p *vs.* pH), and α = 0.5 (irreversible reactions). The amount obtained was 2.19 ± 0.10, indicating the participation of two protons during the oxidation of GLY on the surface of the GrO-PE. The Γ of both CPE and GrO-PE electrodes were estimated using Eq. (3) (considering the geometric area 7.73 × 10^{-2} cm^{-2}), with values obtained of 1.49 × 10^{-11} ± 1.3 × 10^{-12} mol cm^{-2} for CPE and 1.61 × 10^{-10} ± 3.1 × 10^{-12} mol cm^{-2} for GrO-PE. These values indicate that the surface of the GrO-PE adsorbs approximately 11 times more GLY than the CPE does. This difference can be attributed to the presence of GrO in the working electrode.

The standard heterogeneous rate constant (k_s) was determined experimentally using Eq. (4), resulting in values of 5.13 ± 0.17 s^{-1} and 9.86 ± 0.32 s^{-1} for the CPE and GrO-PE respectively. The results obtained for the kinetic parameters of the GLY electrochemical reaction on the surface of the working electrodes show that they were strongly influenced by the presence of the GrO. Finally, after determining the kinetic parameters of the GLY redox reaction on the surface of both working electrodes, the electrochemical reaction of GLY on the CPE and GrO-PE surface was proposed (Fig. 3). First, the protonation of the nitrogen atom of the secondary amine and the deprotonation of the hydroxyl oxygen atom (Fig. 3 Step 1) induces the formation of the deprotonated GLY (GLY–D, Fig. 3). Second, the transfer of electrons between the GLY and the surface of the working electrode shown in Fig. 3 step 2, involving two protons and two electrons, leads to the formation of cyanophosphonic acid and acetic acid (Fig. 3 Step 2). These results support the models already proposed in the literature (Gholivand et al., 2018).

$$n = \frac{2.718RTI_p}{F\nu Q} \quad (1)$$

$$\frac{\Delta E_p}{\Delta pH} = \frac{RTH^+}{\alpha nF} \quad (2)$$

$$\Gamma = \frac{Q}{nFA} \quad (3)$$

$$\log k_s = \alpha \log(1-\alpha) + (1-\alpha)\log\alpha - \log\frac{RT}{nF\nu} - \frac{(1-\alpha)\alpha nF\Delta E_p}{2.3RT} \quad (4)$$

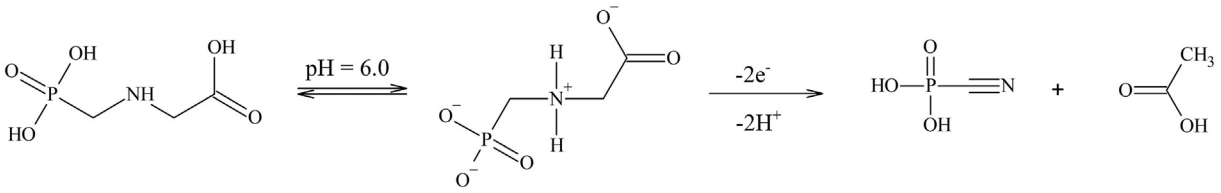

Fig. 3. Possible oxidation reaction of GLY on the surface of CPE and GrO-PE.

3.6. Analytical curve, the limit of detection and quantification

The analytical curve obtained using the GrO-PE sensor under optimized conditions (70 Hz frequency, 40 mV amplitude, 10 mV step potential and pH 6.0) demonstrated good linearity for I_p *vs.* GLY concentration (Fig. 4). The values of LOD and LOQ, determined from the analytical curve by using the methodology described in Section 2.4 (experimental section) are presented in Table 2. A comparison of the results of the analytical performance (concentration range, LOD, and types of samples) of the proposed sensor with results described in the literature is shown in Table 3.

The use of Cu (Gholivand et al., 2018; Aguirre et al., 2019; Cao et al., 2019), Ni (Khenifi et al., 2009) and Au (Noori et al., 2018) electrodes has been reported for the quantitative determination of GLY levels in several types of samples, including water, soil, green vegetables, cucumber, corn, and human serum. The molecular structure of GLY contains functional groups such as amino, carboxyl, and phosphonate, which provide an easier formation of coordination compounds with transition metals (Morillo et al., 1994). These studies utilized the difference between the I_p values of the transition metal oxidation measured in the absence and the presence of GLY as the analytical signal in the electroanalytical determinations. This difference in I_p values arises due to the formation of coordination compounds between GLY and the transition metal previously added to the surface of the working electrode. The reduction of the secondary amine that exists in the molecular structure of GLY leads to the formation of nitrosamines. The compounds formed due to the reduction of GLY can be determined electrochemically and used as an analytical signal due to the electrochemical reduction of GLY–Nitro on the surface of the working electrode.

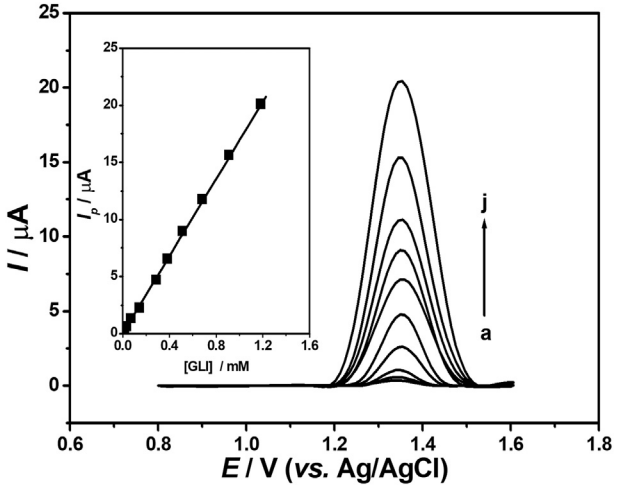

Fig. 4. Voltammograms (SWV) and analytical curve for GLY, using GrO-PE as working electrode. Experimental conditions: BR buffer at 0.2 mol L^{-1} in pH 6.0 [GLY]: a) 1.8×10^{-5}; b) 3.6×10^{-5}; c) 7.2×10^{-5}; d) 1.4×10^{-4}; e) 2.9×10^{-4}; f) 3.8×10^{-4}; g) 5.1×10^{-4}; h) 6.8×10^{-4}; i) 9.1×10^{-4}, and j) 1.2×10^{-3} mol L^{-1}. Frequency: 70 Hz, step: 10 mV and amplitude: 40 mV.

The literature also describes sensors using polypyrrole polymers that had been previously modified with molecularly imprinted AuNPs to determine GLY levels in corn, water, and cucumber samples (Table 3, Xu et al., 2017; Zhang et al., 2017). The analytical signal used to quantify the GLY in these sensors was the difference in the oxidation I_p of $[Fe(CN)_6]^{3+}$ (Xu et al., 2017) ions and the difference in charge transfer resistance of the electrode-solution interface in the presence of iron ions $[Fe(CN)_6]^{3+}$ (Zhang et al., 2017), both in the presence of GLY.

In all the studies on materials employed in electrode modification described above, the electroanalytical determination of GLY occurred indirectly, because it was based on the analytical signal differences due to changes in the transport properties of the electric double layer in the absence and presence of GLY. The analytical performance obtained in this investigation, using the GrO-PE sensor, presented results like those described in the literature (Table 3), based on the direct determination of GLY. In addition, the results obtained for LOD and LOQ (Table 2), shows that the proposed sensor allows the determination of quantities much lower than the maximum allowed residue level (MRL) of GLY in drinking water, according to regulatory agencies such as Health Canada (2019), which sets an MRL of 280 μg L^{-1}, the American Environmental Protection Agency (EPA), which sets an MRL of 700 μg L^{-1} (EPA, n.d.), and the Brazil National Health Surveillance Agency, which sets an MRL of 500 μg L^{-1} (ANVISA, 2018). Therefore, the proposed sensor is robust and can be used to determine GLY traces in environmental samples, since it is sensitive to very low amounts of GLY.

3.7. Precision, repeatability, reproducibility, and selectivity of the GrO-PE

Studies of precision, repeatability, reproducibility, and selectivity were conducted to evaluate the analytical performance of the proposed method (results presented in Fig. 5A and B). I_p and E_p values were obtained from the registered voltammograms in a solution containing 2.2×10^{-5} mol L^{-1} of GLY. The precision, repeatability, and reproducibility of the GrO-PE working electrode showed relative standard deviations (RSDs) of less than 3%, 2%, and 4%, respectively. Examining the effect of potential interferents on the selectivity of the method resulted in RSDs of less than 2%, 3%, and 3% for ions, pesticides, and GDP, respectively. However, environmental samples are susceptible to several types of contaminants and the presence of other compounds with an oxidation potential similar to that of GLY can interfere with the voltammetric response of the sensor and may act as a limiting factor to the proposed method.

Table 2
Analytical parameters obtained from calibration curves for GLY using SWV and GrO-PE (n = 5).

Parameters	Values
Concentration range mol L^{-1}	1.8×10^{-5}–1.2×10^{-3}
Correlation coefficient (±SD)	0.998 ± 0.001
Intercept (±SD) (μA)	0.021 ± 0.001
Slope (±SD) (μA/μmol L^{-1})	0.179 ± 0.004
Limit of detection limit mol L^{-1}	1.7×10^{-8}
Limit of quantification limit mol L^{-1}	5.6×10^{-8}

SD: standard deviation.

Table 3
Studies reporting GLY quantification using electrochemical methods.

Electrodes/methods	Linear range (mol L^{-1})	LOD (mol L^{-1})	Sensor application	Ref.
Cu^{2+}–Cu/GC/DPV	4×10^{-6}–3×10^{-5}	1.9×10^{-7}	Water: distilled and drinking	(Aguirre et al., 2019)
Cu-BTC/ITO/DPV	1×10^{-12}–1×10^{-5}	1.4×10^{-13}	Green vegetable	(Cao et al., 2019)
Electrogenerated NiAl-LDH/films/amperometric	1×10^{-5}–3×10^{-4}	5×10^{-6}	River water	(Khenifi et al., 2009)
AuNPs/PGE//DPV	2.9×10^{-8}–7.7×10^{-6}	2.1×10^{-8}	Water, soil and human serum	(Prasad et al., 2014)
Au/AuNp/MIPP/DPV	2.9×10^{-8}–4.7×10^{-6}	1.6×10^{-9}	Cucumber and tap water	(Zhang et al., 2017)
ITO/AuNp/MIPP/DPV	2.4×10^{-9}–7.1×10^{-9}	5.4×10^{-10}	Corn	(Xu et al., 2017)
CPE/Gly–Is/SWV	4.4×10^{-8}–2.8×10^{-6}	2.0×10^{-9}	Milk, orange juice, and agricultural formulation	(Oliveira et al., 2018)
SPE/Au/Amperometric	3×10^{-4}–2×10^{-3}	1.6×10^{-6}	Water	(Noori et al., 2018)
GrE/MWCNTS/CuO/DPV	5×10^{-9}–1.1×10^{-6}	1.3×10^{-9}	Soil and water	(Gholivand et al., 2018)
GC/MWCNT/CuPc/DPV	8.3×10^{-4}–9.9×10^{-3}	1.19×10^{-5}	Surface waters	(Moraes et al., 2010)
Cu μE/CV	3×10^{-8}–13×10^{-6}	4×10^{-9}	River water	(Regiart et al., 2020)
GrO-PE/SWV	1.8×10^{-5}–1.2×10^{-3}	1.7×10^{-8}	Groundwater, and soybean and lettuce extract.	(This study)

Cu/GC: Cu° electrocrystallization onto glassy carbon. DPV: differential pulse voltammetry. Cu-BTC/ITO: hierarchically porous Cu-BTC. CPE/MWCNT/B: Biosensor based on atemoya peroxidase immobilised on modified nanoclay. CPE/Gly-Is: the isopropylamine salt of glyphosate was determined using CPE. ITO/AuNp/MIPP: AuNPs: Au nanoparticles. Pt/NiAl: Au/AuNPs: gold electrode modified with AuNPs. PGE: pencil graphite electrode. MIPP: molecularly imprinted polypyrrole. AMP: amperometric. ITO: electrodeposited on an indium/tin oxide (ITO) glass. CPE: carbon paste electrode. SWV: square wave voltammetry. SPE: screen-printed electrodes based on gold. GrO-PE: graphite oxide paste electrode. GrE/MWCNTS/CuO: pencil graphite electrode modified by multi-walled carbon nanotube (MWCNTS)-ionic liquid (IL) composite and copper oxide nanoparticle (CuO). GC/MWCNT/CuPc: glassy carbon electrode modified with multi-walled carbon nanotubes plus copper phthalocyanine. Cu μE: bare Cu microelectrode.

The low values of obtained RSD demonstrate that no significant changes were found in the sensor response, indicating that the stability of the developed method is acceptable. Thus, the GrO-PE has high precision, repeatability, reproducibility, and selectivity; it can be used in analytical applications for the quantification of GLY traces in environmental samples.

3.8. Application of the proposed method to groundwater and plants extracts

Our prior investigation of the samples showed that they were free of GLY (Table 4). The aliquots of groundwater and leaf extracts from soybean and lettuce were then spiked with known amounts of GLY (4.9×10^{-7}; $9.3 \times 10^{-7}$and 19.2×10^{-7}) mol L^{-1}. Recovery rates, investigated with GrO-PE, using SWV and the method of standard addition, ranged from 98% to 102% with an RSD of 0.2–2.3% (Table 4). Therefore, the proposed method was successfully applied in the determination of GLY in the tested samples, showing itself to be effective for this purpose.

Table 4
Added and found amounts, relative standard deviations, and recovery rates (n = 3).

Samples	Added ($\times 10^{-7}$ mol L^{-1})	Found ($\times 10^{-7}$ mol L^{-1})	RSD[b] (%)	Recovery (%)	Error[c] (%)
Underground water	0	ND[a]	–	–	–
	4.9	4.8	1.3	97.9	−2.0
	9.3	9.2	2.3	98.9	−1.1
	19.2	19.3	1.8	100.5	+0.5
Soybean extract	0	ND			
	4.9	5.0	1.1	102.1	+2.0
	9.3	9.2	1.5	98.9	−1.1
	19.2	19.3	0.6	100.5	+0.5
Lettuce extract	0	ND			
	4.9	5.0	0.9	102.1	+2.0
	9.3	9.4	0.6	101.1	+1.1
	19.2	19.3	0.2	100.5	+0.5

[a] ND: not detected.
[b] RSD: relative standard deviation, expressed as average of standard deviation × 100, obtained for three replicates of standard addition curves.
[c] Error (%) = [(found value − added value) / (added value)] × 100.

4. Conclusion

In this work, a simple, sensitive, and reliable sensor made from GrO was proposed for the direct determination of GLY traces in environmental samples. The method developed here eliminates laborious modifications of the sensor and GLY derivatization, thus increasing its attractiveness as a more practicable, efficient, and low-cost method. Under optimal conditions for GLY determination, the sensor exhibited a wide linear range

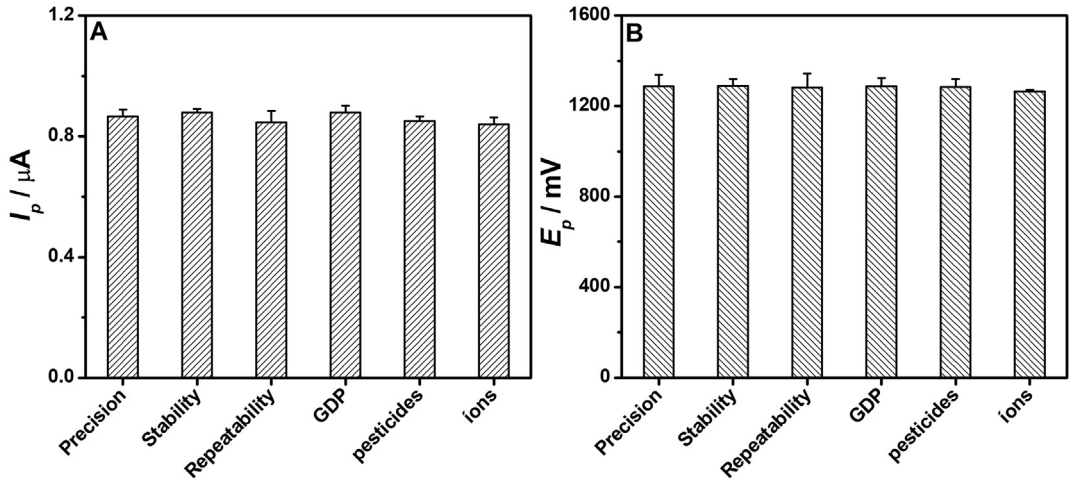

Fig. 5. (A) I_p. (B) E_p. Precision, repeatability, reproducibility, and selectivity, using GrO-PE as the working electrode. Experimental conditions: BR buffer at 0.2 mol L^{-1} in pH 6.0. [GLY] = 2.2×10^{-5} mol L^{-1}. Frequency: 70 Hz, step: 10 mV and amplitude: 40 mV. The initials GDP means glyphosate degradation product.

and low limit of detection. The sensitivity of GrO-PE is associated with the presence of GrO which, through functional groups containing oxygen, provides a greater interaction of the protonated form of GLY with the sensor surface, causing an increase in the electronic transfer constant. With low residual current and stability in the voltammetric response, the electrochemical sensor exhibited excellent precision, repeatability, and reproducibility. In addition, high selectivity was observed since other pesticides, GDP, and ions did not interfere with the sensor response. The practical application was quite satisfactory with high recovery rates in the range of 98% to 102% with an RSD of 0.2–2.3% for the detection of GLY in groundwater as well as leaf extracts from soybean and lettuce. Therefore, the proposed sensor demonstrates great potential for efficiently simplifying the monitoring of GLY traces in environmental samples.

CRediT authorship contribution statement

Conception and design of study: Santos, J. S; Santiago, E. F; Arruda, G. J

Acquisition of data: Santos, J. S; Pontes, M. S

Analysis and/or interpretation of data: Santos, J. S; Fiorucci, A. R; Santiago, E. F; Arruda, G. J

Drafting the manuscript: Santos, J. S; Arruda, G. J

Revising the manuscript critically for important intellectual content: Santos, J. S; Fiorucci, A. R; Santiago, E. F; Arruda, G. J; Pontes, M. S

Approval of the version of the manuscript to be published: Santos, J. S; Fiorucci, A. R; Santiago, E. F; Arruda, G. J; Pontes, M. S.

Declaration of competing interest

The authors declare that they have no known competing financial interests or personal relationships that could have appeared to influence the work reported in this paper.

Acknowledgments

The authors would like to thank the Coordenação de Aperfeiçoamento de Pessoal de Nível Superior (CAPES), by the doctoral scholarship granted to Jaqueline S. Santos (grant number 001), to the Central Analytical Institute of Chemistry of USP of São Carlos, Brazil, by the FTIR. To the Multiuser Laboratory of Materials Analysis (MUTILAM), and to the Institute of Physics of UFMS, Campo Grande Mato Grosso do Sul, by the TGA/DSC and SEM/EDS measurements.

Appendix A. Supplementary data

Supplementary data to this article can be found online at https://doi.org/10.1016/j.scitotenv.2020.142385.

References

Aguirre, M.C., Urreta, S.E., Gomez, C.G., 2019. A Cu^{2+}–Cu/glassy carbon system for glyphosate determination. Sensors Actuators B Chem. 284, 675–683. https://doi.org/10.1016/j.snb.2018.12.124.

ANVISA-Agência Nacional de Vigilância Sanitária- Nota Técnica N° 23/2018/Sei/Creav/Gemar/Ggtox/Dire3/Anvisa.

Bento, C.P.M., Yang, X., Gort, G., Xue, S., Van Dam, R., Zomer, P., Mol, H.G.J., Ritsema, C.J., Geissen, V., 2016. Persistence of glyphosate and aminomethylphosphonic acid in loess soil under different combinations of temperature, soil moisture and light/darkness. Sci. Total Environ. 572, 301–311. https://doi.org/10.1016/j.scitotenv.2016.07.215.

Berman, M.C., Marino, D.J.G., Quiroga, M.V., Zagarese, H., 2018. Occurrence and levels of glyphosate and AMPA in shallow lakes from the Pampean and Patagonian regions of Argentina. Chemosphere 200, 513–522. https://doi.org/10.1016/j.chemosphere.2018.02.103.

Bernal, J., Bernal, J.L., Martin, M.T., Nozal, M.J., Anadón, A., Martínez-Larrañaga, M.R., Martínez, M.A., 2010. Development and validation of a liquid chromatography–fluorescence-mass spectrometry method to measure glyphosate and aminomethylphosphonic acid in rat plasma. J. Chromatogr. B 878, 3290–3296. https://doi.org/10.1016/j.jchromb.2010.10.013.

Cao, Y., Wang, L., Shen, C., Wang, C., Hu, X., Wang, G., 2019. An electrochemical sensor on the hierarchically porous Cu–BTC MOF platform for glyphosate determination. Sensors Actuators B Chem. 283, 487–494. https://doi.org/10.1016/j.snb.2018.12.064.

Cesarino, I., Moraes, F.C., Machado, S.A.S., 2011. A biosensor based on polyaniline-carbon nanotube core-shell for electrochemical detection of pesticides. Electroanalysis 23, 2586–2593. https://doi.org/10.1002/elan.201100161.

Do, M.H., Florea, A., Farre, C., Bonhomme, A., Bessueille, F., Vocanson, F., Nhu-Trang, T.T., Jaffrezic-Renault, N., 2015. Molecularly imprinted polymer–based electrochemical sensor for the sensitive detection of glyphosate herbicide. Int. J. Environ. Anal. Chem. 95, 1489–1501. https://doi.org/10.1080/03067319.2015.1114109.

Franco, D.A.S., Almeida, S.D.B., Cerdeira, A.L., Duke, S.O., Moraes, R.M., Lacerda, A.L.S., Matallo, M.B., 2012. Evaluation of glyphosate application on transgenic soybean and its relationship with shikimic acid. Planta Daninha 30, 659–666. https://doi.org/10.1590/S0100-83582012000300023.

Gao, L., He, J., Xu, W., Zhang, J., Hui, J., Guo, Y., Li, W., Yu, C., 2014. Ultrasensitive electrochemical biosensor based on graphite oxide, Prussian blue, and PTC–NH2 for the detection of α2,6–sialylated glycans in human serum. Biosens. Bioelectron. 62, 79–83. https://doi.org/10.1016/j.bios.2014.06.031.

Gholivand, M.B., Akbari, A., Norouzi, L., 2018. Development of a novel hollow fiber–pencil graphite modified electrochemical sensor for the ultra–trace analysis of glyphosate. Sensors Actuators B Chem. 272, 415–424. https://doi.org/10.1016/j.snb.2018.05.170.

Greef, R., Peat, R., Peter, L.M., Pletcher, D., Robinson, J., 1985. (Southampton Electrochemistry Group): Instrumental Methods in Electrochemistry. Ellis Horwood Ltd., Chichester.

Gurzęda, B., Subrati, A., Florczak, P., Kabacińska, Z., Buchwald, T., Smardz, L., Peplińska, B., Jurga, S., Krawczyk, P., 2020. Two-step synthesis of well-ordered layered graphite oxide with high oxidation degree. Appl. Surf. Sci. 507, 14504. https://doi.org/10.1016/j.apsusc.2019.145049.

Habekost, A., 2014. Rapid and sensitive spectroelectrochemical and electrochemical detection of glyphosate and AMPA with screen–printed electrodes. Talanta 162, 583–588. https://doi.org/10.1016/j.talanta.2016.10.074.

Health Canada, 2019. Guidelines for Canadian Drinking Water Quality-Summary Table. Water and Air Quality Bureau, Healthy Environments and Consumer Safety Branch, Health Canada, Ottawa, Ontario.

IUPAC, 1987. Recommendations for the definition, estimation and use of the detection limit. Analyst 112, 199–204. https://doi.org/10.1039/AN9871200199.

Johansson, H.K.L., Schwartz, C.L., Nielsen, L.N., Boberg, J., Vinggaard, A.M., Bahl, M.I., Svingen, T., 2018. Exposure to a glyphosate–based herbicide formulation, but not glyphosate alone, has only minor effects on adult rat testis. Reprod. Toxicol. 82, 25–31. https://doi.org/10.1016/j.reprotox.2018.09.008.

Khenifi, A., Derriche, Z., Forano, C., Prevot, V., Mousty, C., Scavetta, E., Tonelli, D., 2009. Glyphosate and glufosinate detection at electrogenerated NiAl–LDH thin films. Anal. Chim. Acta 654, 97–102. https://doi.org/10.1016/j.aca.2009.09.023.

Kishore, G.M., Shah, D.M., 1988. Amino acid biosynthesis inhibitors as herbicides. Annu. Rev. Biochem. 57, 627–663.

Kissinger, P.T., Heineman, W.R., 1983. Cyclic voltammetry. J. Chem. Educ. 60, 772. https://doi.org/10.1021/ed060p702.

Mercurio, P., Flores, F., Mueller, J.F., Carter, S., Negri, A.P., 2014. Glyphosate persistence in seawater. Mar. Pollut. Bull. 85, 385–390. https://doi.org/10.1016/j.marpolbul.2014.01.021.

Moraes, F.C., Mascaro, L.H., Machado, S.A., Brett, C.M., 2010. Direct electrochemical determination of glyphosate at copper phthalocyanine/multiwalled carbon nanotube film electrodes. Electroanalysis 22, 1586–1591. https://doi.org/10.1002/elan.200900614.

Morillo, E., Maqueda, C., Bejarano, M., Madrid, L., Undabeytia, T., 1994. Cu (II)–glyphosate system: a study by anodic stripping voltammetry and the influence on Cu adsorption by montmorillonite. Chemosphere 28, 2185–2196. https://doi.org/10.1016/0045-6535(94)90186-4.

Motojyuku, M., Saito, T., Akieda, K., Otsuka, H., Yamamoto, I., Inokuchi, S., 2008. Determination of glyphosate, glyphosate metabolites, and glufosinate in human serum by gas chromatography–mass spectrometry. J. Chromatogr. B 875, 509–514. https://doi.org/10.1016/j.jchromb.2008.10.003.

Noori, J., Dimaki, M., Mortensen, J., Svendsen, W., 2018. Detection of glyphosate in drinking water: a fast and direct detection method without sample pretreatment. Sensors 18, 2961–2969. https://doi.org/10.3390/s18092961.

Okada, E., Costa, J.L., Bedmar, F., 2016. Adsorption and mobility of glyphosate in different soils under no-till and conventional tillage. Geoderma 263, 78–85. https://doi.org/10.1016/j.geoderma.2015.09.009.

Oliveira, P.C., Maximiano, E.M., Oliveira, P.A., Camargo, J.S., Fiorucci, A.R., Arruda, G.J., 2018. Direct electrochemical detection of glyphosate at carbon paste electrode and its determination in samples of milk, orange juice, and agricultural formulation. J. Environ. Sci. Health B 53, 817–823. https://doi.org/10.1080/03601234.2018.1505081.

Petroni, J.M., Lucca, B.G., Ferreira, V.S., 2017. Simple and inexpensive electrochemical platform based on novel homemade carbon ink and its analytical application for determination of nitrite. Electroanalysis 29, 1762–1771. https://doi.org/10.1002/elan.201700117.

Ping, J., Wang, Y., Fan, K., Wu, J., Ying, Y., 2011. Direct electrochemical reduction of graphene oxide on ionic liquid doped screen-printed electrode and its electrochemical biosensing application. Biosens. Bioelectron. 28, 204–209. https://doi.org/10.1016/j.bios.2011.07.018.

Ping, J., Wu, J., Wang, Y., Ying, Y., 2012. Simultaneous determination of ascorbic acid, dopamine and uric acid using high-performance screen-printed graphene electrode. Biosens. Bioelectron. 34, 70–76. https://doi.org/10.1016/j.bios.2012.01.016.

Ping, J., Wang, Y., Wu, J., Ying, Y., 2014. Development of an electrochemically reduced graphene oxide modified disposable bismuth film electrode and its application for stripping analysis of heavy metals in milk. Food Chem. 151, 65–71. https://doi.org/10.1016/j.foodchem.2013.11.026.

Ping, J., Zhou, Y., Wu, Y., Papper, V., Boujday, S., Marks, R.S., Steele, T.W., 2015. Recent advances in aptasensors based on graphene and graphene-like nanomaterials. Biosens. Bioelectron. 64, 373–385. https://doi.org/10.1016/j.bios.2014.08.090.

Prasad, B.B., Jauhari, D., Tiwari, M.P., 2014. Doubly imprinted polymer nanofilm–modified electrochemical sensor for ultra–trace simultaneous analysis of glyphosate and glufosinate. Biosens. Bioelectron. 59, 81–88. https://doi.org/10.1016/j.bios.2014.03.019.

Regiart, M., Kumar, A., Gonçalves, J.M., Silva Junior, G.J., Masini, J.C., Angnes, L., Bertotti, M., 2020. An electrochemically synthesized nanoporous copper microsensor for highly sensitive and selective determination of glyphosate. ChemElectroChem 7, 1558. https://doi.org/10.1002/celc.202000064.

Royer, A., Beguin, S., Tabet, J.C., Hulot, S., Reding, M.A., Communal, P.Y., 2000. Determination of glyphosate and aminomethylphosphonic acid residues in water by gas chromatography with tandem mass spectrometry after exchange ion resin purification and derivatization. Application on vegetable matrixes. Anal. Chem. 72, 3826–3832. https://doi.org/10.1021/ac000041d.

Santos, J.S., Pontes, M.S., Grillo, R., Fiorucci, A.R., Arruda, G.J., Santiago, E.F., 2020. Physiological mechanisms and phytoremediation potential of the macrophyte *Salvinia biloba* towards a commercial formulation and an analytical standard of glyphosate. Chemosphere 127417. https://doi.org/10.1016/j.chemosphere.2020.127417.

Sato, K., Jin, J.Y., Takeuchi, T., Miwa, T., Suenami, K., Takekoshi, Y., Kanno, S., 2001. Integrated pulsed amperometric detection of glufosinate, bialaphos and glyphosate at gold electrodes in anion–exchange chromatography. J. Chromatogr. A 919, 313–320. https://doi.org/10.1016/S0021-9673(01)00843-3.

Sprankle, P., Meggitt, W.F., Penner, D., 1975. Adsorption, mobility, and microbial degradation of glyphosate in the soil. Weed Sci. 23, 229–234. https://doi.org/10.1017/S0043174500052929.

USEPA, d. Edition of the Drinking Water Standards and Health Advisories. United States Environmental Protection Agencyhttp://www.epa.gov.

Van Stempvoort, D.R., Roy, J.W., Brown, S.J., Bickerton, G., 2014. Residues of the herbicide glyphosate in riparian groundwater in urban catchments. Chemosphere 95, 455–463. https://doi.org/10.1016/j.chemosphere.2013.09.095.

Velasco, J.G., 1997. Determination of standard rate constants for electrochemical irreversible processes from linear sweep voltammograms. Electroanalysis 9, 880–882. https://doi.org/10.1002/elan.1140091116.

William, S., Hummers, J.R., Richard, E., Offeman, 1958. Preparation of graphitic oxide. J Am Chem Soc 80, 1339. https://doi.org/10.1021/ja01539a017.

Wong, A., Santos, A.M., Baccarin, M., Cavalheiro, É.T.G., Fatibello-Filho, O., 2019. Simultaneous determination of environmental contaminants using a graphite oxide–polyurethane composite electrode modified with cyclodextrin. Mater. Sci. Eng. C 99, 1415–1423. https://doi.org/10.1016/j.msec.2019.02.093.

Xu, J., Zhang, Y., Wu, K., Zhang, L., Ge, S., Yu, J., 2017. A molecularly imprinted polypyrrole for ultrasensitive voltammetric determination of glyphosate. Microchim. Acta 184, 1959–1967. https://doi.org/10.1007/s00604-017-2200-9.

Yang, X., Lwanga, E.H., Bemani, A., Gertsen, H., Salanki, T., Guo, X., Fu, H., Xue, S., Ritsema, C., Geissen, V., 2019. Biogenic transport of glyphosate in the presence of LDPE microplastics: a mesocosm experiment. Environ. Pollut. 245, 829–835. https://doi.org/10.1016/j.envpol.2018.11.044.

Yao, Y., Ping, J., 2018. Recent advances in graphene-based freestanding paper-like materials for sensing applications. TrAC, Trends Anal. Chem. 105, 75–88. https://doi.org/10.1016/j.trac.2018.04.014.

Yao, Y., Jiang, C., Ping, J., 2019. Flexible freestanding graphene paper-based potentiometric enzymatic aptasensor for ultrasensitive wireless detection of kanamycin. Biosens. Bioelectron. 123, 178–184. https://doi.org/10.1016/j.bios.2018.08.048.

Zelaya, I.A., Anderson, J.A., Owen, M.D., Landes, R.D., 2011. Evaluation of spectrophotometric and HPLC methods for shikimic acid determination in plants: models in glyphosate–resistant and–susceptible crops. J. Agric. Food Chem. 59, 2202–2212. https://doi.org/10.1021/jf1043426.

Zhang, Y., Zhang, Y., Qu, Q., Wang, G., Wang, C., 2013. Determination of glyphosate and aminomethylphosphonic acid in soybean samples by high performance liquid chromatography using a novel fluorescent labeling reagent. Anal Methods 5, 6465–6472. https://doi.org/10.1039/c3ay41166d.

Zhang, C., She, Y., Li, T., Zhao, F., Jin, M., Guo, Y., Zheng, L., Wang, S., Jin, F., Shao, H., Liu, H., Wang, J., 2017. A highly selective electrochemical sensor based on molecularly imprinted polypyrrole–modified gold electrode for the determination of glyphosate in cucumber and tap water. Anal. Bioanal. Chem. 409, 7133–7144. https://doi.org/10.1007/s00216-017-0671-5.

Zhao, J., Pacenka, S., Wu, J., Richards, B.K., Steenhuis, T., Simpson, K., Hay, A.G., 2018. Detection of glyphosate residues in companion animal feeds. Environ. Pollut. 243, 1113–1118. https://doi.org/10.1016/j.envpol.2018.08.100.